

Controlling Soft Robots

Balancing Feedback and Feedforward Elements

© PHOTOCREDIT

By Cosimo Della Santina, Matteo Bianchi, Giorgio Grioli, Franco Angelini, Manuel Catalano, Manolo Garabini, and Antonio Bicchi

Soft robots (SRs) represent one of the most significant recent evolutions in robotics. Designed to embody safe and natural behaviors, they rely on compliant physical structures purposefully designed to embody desirable and sometimes variable impedance characteristics. This article discusses the problem of controlling SRs. We start by observing that most of the standard methods of robotic control—e.g., high-gain robust control, feedback linearization, backstepping, and active impedance control—effectively fight against or even completely cancel the physical dynamics of the system, replacing them with a desired model. This defeats the purpose of introducing physical compliance. After all, what is the point of building soft actuators if we then make them stiff by control?

An alternative to such approaches can be conceived by observing humans, who can obtain good motion accuracy and repeatability while maintaining the intrinsic softness of their bodies. In this article, we show that an anticipative model of human motor control, using a feedforward action combined with low-gain feedback, can be used to achieve human-like behavior. We present an implementation of such an idea that uses iterative learning control. Finally, we present the experimental results of the application of such learned anticipative control to a physically compliant robot. The control application achieves the desired behavior much better than a classical feedback controller used for comparison.

Quest for Good SR Performance

The term *SR* refers to a robotic system that exhibits compliant interactions with the external world. SRs are often designed to embody natural behaviors, such as smooth movements, energy efficiency, resilience, and safety. Often, the design of an SR is inspired by natural human or animal models. The

Digital Object Identifier 10.1109/MRA.2016.2636360
Date of publication: 17 May 2017

development of this new generation of robots explicitly targets two main problems: 1) guaranteeing optimized performance and increased effectiveness in the accomplishment of tasks, e.g., very dynamic tasks, and 2) enabling a safe interaction with the environment and with coexisting humans. The formal framework for the solution of the latter problem was notoriously established by Hogan in [15]. To achieve these goals, it is crucial that the robot exhibit a high degree of compliance, elasticity, and damping—i.e., a suitable mechanical impedance. This can be achieved actively, e.g., through torque control at the joint level, or passively, i.e., via the physical characteristics of the robot's component materials. The latter approach has attracted growing attention in recent years for a number of advantages it offers. Examples are serial elastic actuators (SEAs) [34] and variable-stiffness actuators (VSAs) [40]. Another large class of SRs comprises those that incorporate continuously deformable mechanical structures, such as trunks or tentacles (for an extensive review of these systems, see, e.g., [22]).

From a control point of view, much effort has been devoted to developing SR control strategies to guarantee optimized performance. For instance, in [1] a numerical framework for simultaneous optimization of torque and stiffness incorporating real-world constraints is proposed. In [11], the problem of optimizing motion and stiffness to maximize the impact of a VSA-actuated hammer is analytically addressed and experimentally demonstrated. As previously mentioned, physically compliant elements are deliberately introduced in SR designs to achieve desirable behaviors. This approach can often be regarded as so-called intelligence embodying in robots' physical structure. Alternatively, it can be described as providing a degree of morphological computation [33].

When it comes to compliant control systems, however, it turns out that achieving performance is not at all easier. This fact is intuitive for such measures of performance as positional accuracy, which is the reason industrial robots have traditionally been built for maximum rigidity. It is also true for other tasks, however, including conventional force control, as illustrated with great simplicity by the classic results in, e.g., [9]. To achieve acceptable SR performance, approaches involving higher control authority (e.g., high-gain robust control) and/or more sophisticated control techniques (such as feedback linearization, backstepping, and active impedance control) could be used. However, in this article we show how these approaches deeply affect the behavior of the robot, replacing their natural dynamics with a different desired model that makes them stiffer.

An Elementary Example

Consider one of the simplest soft mechanisms, consisting of an elastic element connecting a link of mass m to an actuator (Figure 1). Assume for simplicity that the actuator is accurately controlled, so that its reference position θ can be assumed to be the actual input to the series elastic connection. The dynamic model for the link motion $q(t)$ is thus simply

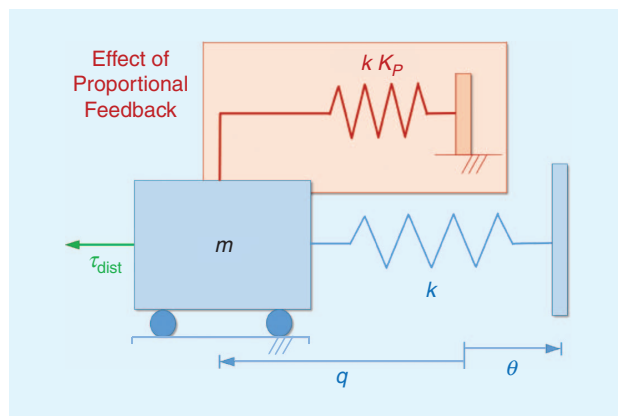


Figure 1. An elementary model of an SEA used to illustrate how feedback alters designed softness. In an open loop, the interface with the environment has the same stiffness k as the physical spring. Closed-loop control with proportional feedback action K_p , however, is tantamount to introducing a second spring of stiffness kK_p in parallel.

$$m\ddot{q} + \beta\dot{q} + kq = k\theta + \tau_{\text{dist}}, \quad (1)$$

where β and k are the physical damping and stiffness of the elastic element, respectively, while the force τ_{dist} represents nonmodeled dynamics and external disturbances. To compensate for τ_{dist} and regulate the link position q , a basic control law is $\theta = -K_p q - K_d \dot{q}$, from which directly comes the closed-loop dynamics

$$m\ddot{q} + \beta\left(1 + \frac{k}{\beta}K_d\right)\dot{q} + k(1 + K_p)q = \tau_{\text{dist}}. \quad (2)$$

As is to be expected from elementary control considerations, the performance of this regulator for promptness and disturbance rejection (both at steady state and in H_∞ norm) monotonically increases with gain K_p (Figure 2). However, from (2), it is also clear that with this feedback

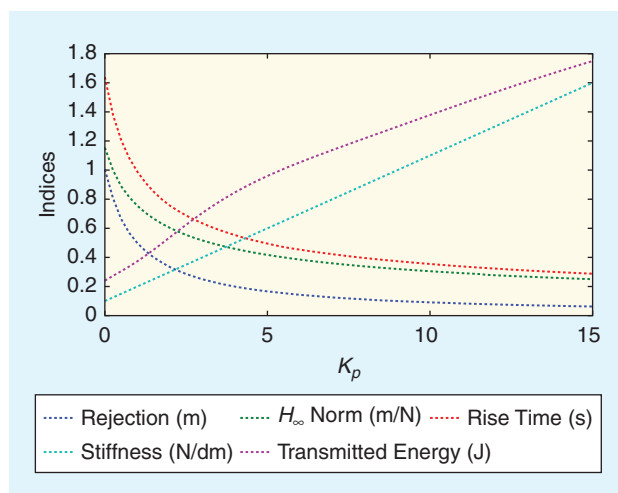


Figure 2. With the growth of the proportional feedback action K_p , the controlled SEA system improves its regulation performance but also increases its stiffness and energy transfer. Data are obtained with $m = 1$ kg, $\beta = 1$ (Ns/m), $k = 1$ (N/m), and $K_d = 0$ s.

action the natural stiffness and damping are amplified by factors $1 + K_p$ and $1 + k/\beta K_d$, respectively (compare Figure 2). In other words, regulation (and tracking) performance is obtained in feedback at the price of stiffening the SR. In the following section, we generalize the idea illustrated in this elementary example for a nonlinear mechanical system, controlled through a generic nonlinear controller.

Feedback Control of SRs

Here, we consider the effect of a generic feedback control action on the stiffness of an SR. We first consider algebraic state feedback methods, which include, e.g., proportional-derivative control, linear quadratic regulator (LQR), computed torque, active impedance control, feedback linearization, and Lyapunov control. For a general overview of the application to robots of many of these control methods, refer to [36]. Applications of these techniques to SRs are discussed in, e.g., [32] and [38].

It is intuitively clear that many of these control techniques strongly modify the mechanical stiffness, since most of them operate a cancellation of the system dynamics. However, we provide a more detailed analytic argument. Consider a generic Lagrangian mechanical system, with the simplifying assumptions that the motor dynamics are negligible and that the spring characteristics depend on the deflection (i.e., the difference between the actual position q and the reference position θ) and possibly on an additional parameter, denoted here as σ , to represent, e.g., the command used in VSAs to set joint stiffness.

Let $T(q - \theta, \sigma)$ denote the vector collecting the torques due to compliant elements at different joints. Considering that stiffness, in a general nonlinear elastic system, can be defined only locally, we take stiffness to be the derivative of torque with regard to the Lagrangian variables, i.e., $\partial T/\partial q$. To formalize the idea of minimizing the physical compliance alteration is to require that the stiffness value in closed loop remains in a δ -neighborhood of the value in the open loop all along the nominal system trajectories, i.e., when the deflection is null $q = \theta$, as follows:

$$\left\| \frac{\partial T(q - \theta, \sigma)}{\partial q} \Big|_{q=\theta} - \frac{\partial T(q - \psi(q, \dot{q}, t, \sigma, r), \sigma)}{\partial q} \Big|_{q=\bar{q}} \right\| \leq \delta, \quad (3)$$

where $\psi(q, \dot{q}, t, \sigma, r)$ is a generic algebraic controller, \bar{q} is a fixed point of ψ (i.e., $\psi(\bar{q}) = \bar{q}$), and the matrix 2-norm is used. Note that the considered control can comprehend, e.g., any combination of feedback (thanks to the q, \dot{q} dependence) and feedforward (thanks to the t, σ, r dependence). Notice also that the same holds for a more general a torque characteristic of type $T(q - r, \sigma) + G(q)$, with $G(q)$ being a generic function of q , e.g., describing gravity effects on stiffness [16]. Furthermore, impedance can be considered instead of stiffness by adding the derivatives with regard to \dot{q}, \ddot{q} .

The following sufficient condition to fulfill (3) can be derived as

$$\left\| \frac{\partial \psi(q, \dot{q}, t, \sigma, r)}{\partial q} \Big|_{q=\bar{q}} \right\| \leq \delta \left\| \frac{\partial T}{\partial q}(0, \sigma) \right\|^{-1}, \quad (4)$$

where $(\partial \psi/\partial q)$ is the proportional component of the control action, and $(\partial T/\partial q(0, \sigma))$ is the natural stiffness along system trajectories, playing the role of a normalization constant.

Inequality (4) means that, to preserve the natural softness characteristic, the proportional component of the feedback has to be sufficiently small, or even null if we request no stiffness alteration (i.e., $\delta = 0$).

Condition (4) can be generalized to the class of nonlinear dynamical controller, considering a feedback action $\theta = \psi(q, \dot{q}, t, \sigma, r, p)$, where p is the state of the dynamic part, evolving according to $\dot{p} = \Pi(q, \dot{q}, t, \sigma, r, p)$. Similar considerations as those above yield the condition

$$\left\| \frac{\partial \psi}{\partial q} + \frac{\partial \psi}{\partial p} \frac{\partial p}{\partial q} \Big|_{q=\bar{q}} \right\| \leq \delta \left\| \frac{\partial T}{\partial q}(0, \sigma) \right\|^{-1}, \quad (5)$$

where dependence of ψ and p is omitted for the sake of readability. Therefore, the dynamic feedback of the Lagrangian variables q also alters the mechanical stiffness of the system.

To clarify the contribution of the term $\partial p/\partial q_i$, we refer to control systems with linear dynamics. It is worth noticing that such a class of controllers includes many typically used in robotic control practice, such as proportional integrative derivative controller, μ -control, and nonlinear output tracking [28]. Since these controllers are integrable in closed form, the term can be expressed explicitly, obtaining

$$\frac{\partial p}{\partial q_i} = \int_0^t e^{A(t-\tau)} B \frac{\partial u(\tau)}{\partial q_i} dt, \quad (6)$$

where A is the dynamic matrix of the control system, B is its input matrix, and $u = [q, \dot{q}, t, \sigma, r]$ is the controller input.

Therefore, in the dynamic case, the resulting closed-loop stiffness becomes time varying. Note that $\partial u(\tau)/\partial q_i$ is a vector with all elements equal to zero, except for the one corresponding to q_i . It follows that $\partial p/\partial q_i$ is the unitary step response of the control system.

To summarize, we have shown that there is a fundamental link between feedback gain, tracking performance, and stiffness variation that applies to all feedback controllers.

Control with Limited Feedback

The results derived in the previous section illustrate that to obtain good tracking performance, feedback control imposes de facto a reduction in the compliance of the controlled mechanism. This contrasts with observations of human motor control. Indeed, the musculoskeletal structure of humans and most vertebrates is composed of considerably softer materials than most current robots. Humans do alter

the stiffness of their body parts through cocontraction of groups of antagonistic muscles. However, we use this sparingly, mainly when we expect unpredictable external forces to disturb our equilibrium [25]. It has also been observed that humans use higher stiffness in the learning phases of a new motor task [30], while with training we reduce cocontraction to a bare minimum.

Another interesting fact is that humans are able to rapidly learn new motor control patterns in changing environmental conditions, requiring different stiffness settings. This has been elucidated in a series of important papers (see, e.g., [21], [23], and [24]) that have shown how subjects adapt their motor control scheme to counter disturbing forces within only a few trials.

The observations of human motor control summarized here have prompted a wide interest in models that explain how humans are able to achieve very good accuracy without sacrificing the natural softness of their musculoskeletal system. A vast literature, reviewed, e.g., in [41], converges on the thesis that human motor performance is achieved through the interaction of two main components: one that is reactive and the other anticipatory. The reactive control component involves the use at different levels in the nervous system of sensory inputs to update ongoing motor commands, which in control language can be referred as *feedback* action. The anticipatory component exploits the ability to predict the consequences of motor events, based on sensorimotor memory and internal models [21], to select in advance which motor command will lead to accomplishing a given task under the foreseeable conditions. The existence and roles of anticipatory and reactive control have been highlighted in many different motor control tasks, including grasping and manipulation ([10], [18], [19], dynamic vision [13], ball catching [26], and locomotion [39]).

In automatic control terminology, anticipatory and reactive control components translate directly to feedforward and feedback actions, respectively. While traditionally more attention has been focused on feedback control, feedforward policies have also been studied, in particular in the field of optimal control. In recent years, the availability of computational power to rapidly recompute optimal feedforward plans in correspondence with sensed changes of state has enabled the application of model predictive control techniques [27]. The fundamental performance limitations of feedback control in the presence of noisy channels have been thoroughly studied in [29]. Feedforward control has become an important tool to address problems in networked control with bandwidth limitations (compare [14]) and with packet-switching induced delays [12] as well as in applications where sensing is difficult, as in micro- and nanoscale positioning (see, e.g., [6]).

In [3] and [4], Roger Brockett proposed an interesting formulation of an optimal control problem that attempts to model how to merge feedforward and feedback components to achieve a minimum attention control (MAC). Indicating with $u(x, t)$ the control function dependence

from the current state x and time t , an attention function is proposed as

$$\eta = \int_{\mathbb{R}^n} \int_0^\infty (1 - \alpha) \left\| \frac{\partial u}{\partial x} \right\|^2 + \alpha \left\| \frac{\partial u}{\partial t} \right\|^2 dt dx,$$

with α a relative weight of the feedforward component $\partial u/\partial t$ with respect to the feedback component $\partial u/\partial x$. To this formulation, a boundary constraint that $u(x, t)$ stabilizes the system along the desired trajectory has to be added. A numerical solution of the MAC problem for a robotic ball-catching example is described in [17]. While the general MAC problem is very complex and a comprehensive solution has yet to be found, it does suggest a model of how a progressively better learned feedforward/anticipative action can relieve the need of a strong feedback/reactive action to achieve fast and accurate movements.

Leveraging such insights to overcome the limitations described in the “Feedback Control of SRs” section, we consider control of SRs combining relatively mild feedback gains with a suitable feedforward action. According to the latter section’s results, specifically (4), the anticipatory components of ψ depend on t, σ, r but not on q , so that $\partial \psi_i / \partial q_i \equiv 0$. Hence, feedforward control does not alter the natural robot softness.

Clearly, the usefulness of feedforward actions depends on the availability of a good model of the system, including the robot and its environment (see, e.g., [7]). Because such a model is rarely available in practice, alternative techniques for developing good anticipatory control are needed. A natural approach that is viable in some applications is to proceed by trials, i.e., by successive approximations of increasing quality—in other words, by learning the controller using performance as a reward.

The machine-learning approach to feedforward design, which is attracting considerable attention in the literature (see, e.g., [35] for an extensive review), can be summarized as an attempt at reconstructing complete models of the robotic system by collecting and regressing large amounts of data. A somewhat different approach comes from the above-mentioned human observations. The human nervous system appears to be able to learn the feedforward action needed to control an unknown dynamic system along a trajectory through several repetitions of the same tracking task [37]. Figure 3 represents a classical experiment in which the subject is asked to reach some points in the workspace. Then a force field is introduced. Initially, trajectories are strongly deformed by the field, but after repetitions of the same movement, the performance obtained before the introduction of the force field can again be achieved.

In [8], Emken et al. present a model of this learning process by repetition of the same action, derived from a statistical model of error evolution over iterations:

$$\theta^{i+1} = f\theta^i + \alpha e^i, \quad (7)$$

where f, α are two constants, and $\theta^i: [t_0, t_f] \rightarrow \mathbb{R}^m$ and $e^i: [t_0, t_f] \rightarrow \mathbb{R}^m$ are the whole control action and error

evolution, respectively, at the i th iteration. In this way, an input sequence is iteratively found such that the output of the system is as close as possible to a desired output. Iterative Learning Control [2] (ILC) permits embedding this rule in a

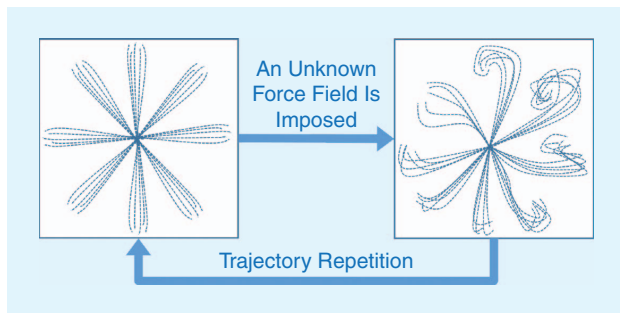


Figure 3. A representation of a typical human motor-control experiment. A subject is able to reach a series of points in space with a hand (trajectories in the left box). When a force field is imposed, e.g., through a haptic interface, the trajectories are deformed (right box). After repeating the reaching trials many times, the subject is able to restore the initial behavior.

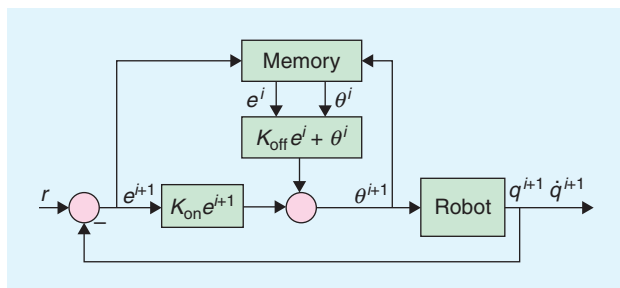


Figure 4. A block scheme of the considered algorithm with the main quantities noted. The reference is r , q^{i+1} and \dot{q}^{i+1} are the system state, and e^i and e^{i+1} are the tracking errors at the previous and the current iterations, respectively. The control inputs at the previous and the current iterations are θ^i, θ^{i+1} , respectively. The memory block stores the error and the control action from the previous iteration of the task.

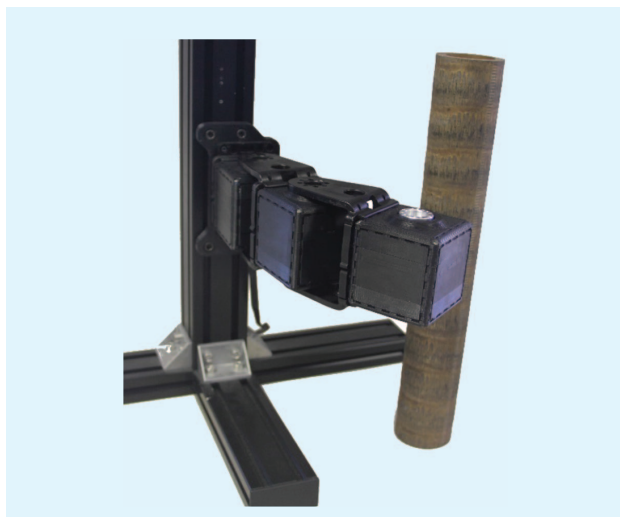


Figure 5. The experimental setup: a two-degrees of freedom (DoF) horizontal VSA arm built using Qbmove Maker Pro servo motors and a bar as an environmental constraint.

general theory. ILC exploits the error evolution of the whole interval $[t_0, t_f]$ of a previous iteration to update a feedforward command, according to the law

$$\theta^{i+1} = Q(\theta^i) + R(e^i), \quad (8)$$

where the function $R(e^i)$ identifies the ILC algorithm, and $Q(\theta^i)$ is a function that maps the old control in the new one (typically a smoothing function). It is interesting to note that there is evidence (e.g., reported in [20]) that in humans feedback motor correction plays a crucial role in motor learning. Hence, a more general algorithm able to merge all these contributions should be considered. Leveraging this observation, we can take advantage of the ILC literature rewriting the control law (8), as in the so-called current-iteration ILC [2],

$$\theta^{i+1} = Q(\theta^i) + R(e^i, e^{i+1}), \quad (9)$$

where the presence of e^{i+1} permits incorporating the feedback action in the same framework. In this manner, ILC can be used to design an appropriate algorithm that permits learning the feedforward action in a human-like manner.

To illustrate the application of the ILC framework to an SR, we use in the following a combination of current-state ILC and LQR feedback. The control law [of type (9)] is

$$\theta^{i+1} = Q(\theta^i) + K_{off} e^i + K_{on} e^{i+1}, \quad (10)$$

where θ^i, e^i are the control action and the error at the i -th iteration. $Q(\cdot)$ is a suitable average mean filter, and K_{off}, K_{on} are two linear gains. Figure 4 shows the block diagram of the algorithm. For this control law, (4) becomes

$$\|K_{on}\| \leq \delta \left\| \frac{\partial T}{\partial q}(0, \sigma) \right\|^{-1}. \quad (11)$$

Hence, it is always possible to choose K_{on} such that (4) is satisfied. Here K_{on} is the result of an LQR and K_{off} is such that the condition in [31] is fulfilled. Further technicalities concerning the particular choice of K_{off}, K_{on} will be discussed in future works.

Experimental Results

In the following, we report an experimental example that aims to show the concepts previously mentioned: 1) alteration of mechanical stiffness due to high-gain feedback and 2) the effectiveness of the control law (10) in stiffness conservation (i.e., in presenting an anticipatory behavior).

In this experiment, we used the setup in Figure 5. The experiments were performed using Qbmove Maker Pro [5] actuators as a test bed. These are modular, variable-stiffness servos based on an agonist-antagonist mechanism. Using this modular system, we built a VSA revolute revolute planar arm. First, we used a purely high-gain proportional integral integral (PII) feedback control to track the trajectory, while the natural stiffness was set to be low. Then we ran the ILC algorithm to teach the robot

to follow the desired trajectory on the horizontal plane, with both low and high constant stiffness. θ^0 was chosen through the inversion of a simplified model of the SR. Finally, in all three cases, we placed a brass bar next to the robot in such a way that impact with it was unavoidable. The goal was to track the trajectory while maintaining the natural behavior of the robot in different configurations. I.e., we expected that the robot would push over the bar if the joints were stiff, and would gently comply with its presence if the joints were soft.

Figure 6 presents the integral of the 2-norm of the tracking error (normalized by the terminal time) at each iteration, in experiments without impacts. The accuracy of the pure high-gain feedback control scheme on the soft configuration is also reported for comparison. The iterative learning law (10) is applied to the robot in its high and low physical stiffness configurations. The results show an increasingly better tracking by the learning controller, with an accuracy of the SR that converges toward that achieved with the stiff robot, while both eventually overcome the accuracy of the high-gain feedback. Photographic sequences illustrating the execution of the final (150th) iteration of the ILC on the stiff robot, the ILC on the SR, and the high-gain PII on the SR are reported in (a)–(c) of Figures 7, 8, and 9, respectively.

Figures 7–9 (d)–(f) show the effect of an impact with the brass bar under the same conditions. When the mechanical stiffness of the robot is set to high, the robot knocks the bar down [Figure 7(d)–(f)] as it continues on to track the reference trajectory, as expected. When the mechanical stiffness is low, but the high-gain PII controller is used, the bar is also pushed over [Figure 8(d)–(f)]. However, as shown in Figure 9(d)–(f), the ILC controller makes it so that the robot preserves its natural compliance and has a very moderate impact with the bar. Figure 10 provides a more precise description of these behaviors in terms of the actual trajectories followed by the first and second robot joints before and after the impact.

Finally, in Figures 11 and 12 we show the total amount of feedforward and feedback exerted by the algorithm to control the system. The relative weight of the total control attention is gradually shifted from the feedback to the feedforward components during the learning phase of the ILC scheme. The motivation for this behavior is twofold: on one side, the feedforward action, which is initialized with a low value, is progressively more authoritative. Perhaps more important, the feedback action is less and less needed over time, as the improving results of learning result in fewer and fewer errors to compensate for (as shown in Figure 6).

Conclusions

In this work, we discussed a fundamental contradiction in the feedback control of SRs, i.e., to obtain good accuracy high gain is needed, which in turn destroys the purposely introduced softness. If feedback control alone is applied to an SR, it may thus alter its natural behavior to something different than what was chosen in the design. We also

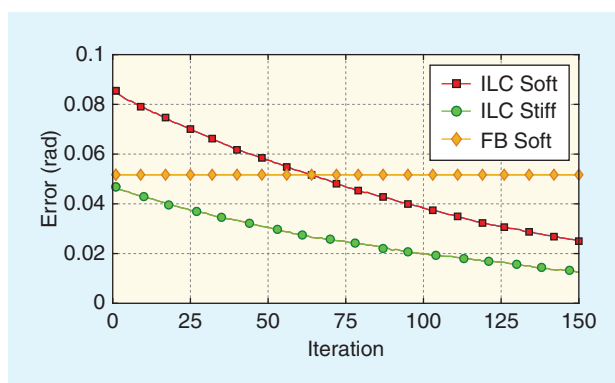


Figure 6. The time integral of the experimental error at each iteration, normalized by the terminal time. The results refer to the low- and high-stiffness cases with the ILC algorithm and to the soft case with the PII. FB: feedback.

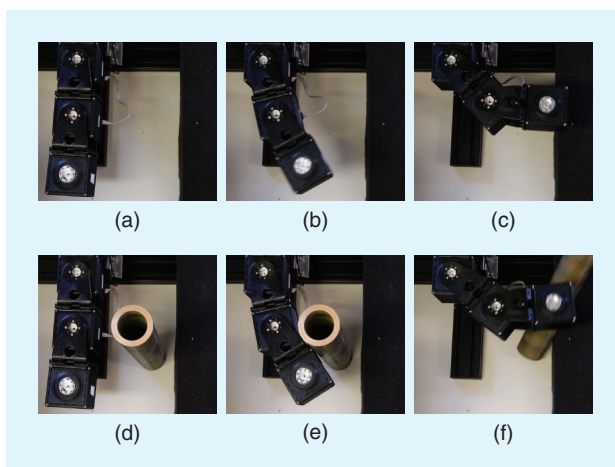


Figure 7. The evolution resulting from the application of the ILC algorithm with high stiffness: robot positions (without an obstacle) at (a) $t = 0$ s, (b) $t = 1$ s, and (c) $t = 2$ s, and (with an obstacle) at (d) $t = 0$ s, (e) $t = 1$ s, and (f) $t = 2$ s. With an obstacle present, the robot drops the bar.

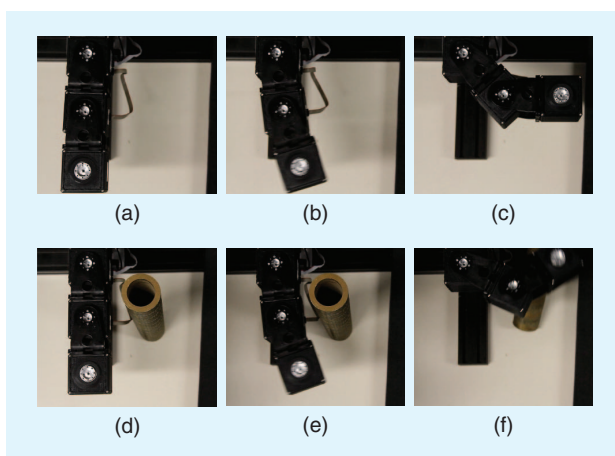


Figure 8. The evolution resulting from the application of high gain feedback with low stiffness: robot positions (without an obstacle) at (a) $t = 0$ s, (b) $t = 1$ s, and (c) $t = 2$ s, and (with an obstacle) at (d) $t = 0$ s, (e) $t = 1$ s, and (f) $t = 2$ s. With an obstacle present, the robot drops the bar, as in the stiff case.

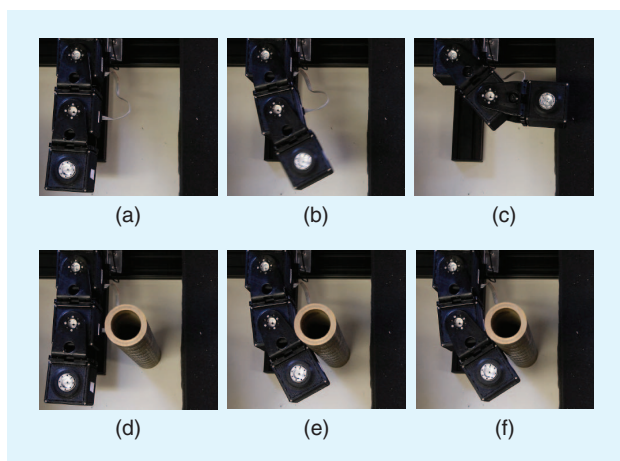


Figure 9. The evolution resulting from the application of the ILC algorithm with low stiffness: robot positions (without an obstacle) at (a) $t = 0$ s, (b) $t = 1$ s, and (c) $t = 2$ s, and (with an obstacle) at (d) $t = 0$ s, (e) $t = 1$ s, and (f) $t = 2$ s. With an obstacle present, the robot adapts to the external environment (i.e., the mechanical stiffness is preserved by the proposed anticipatory control).

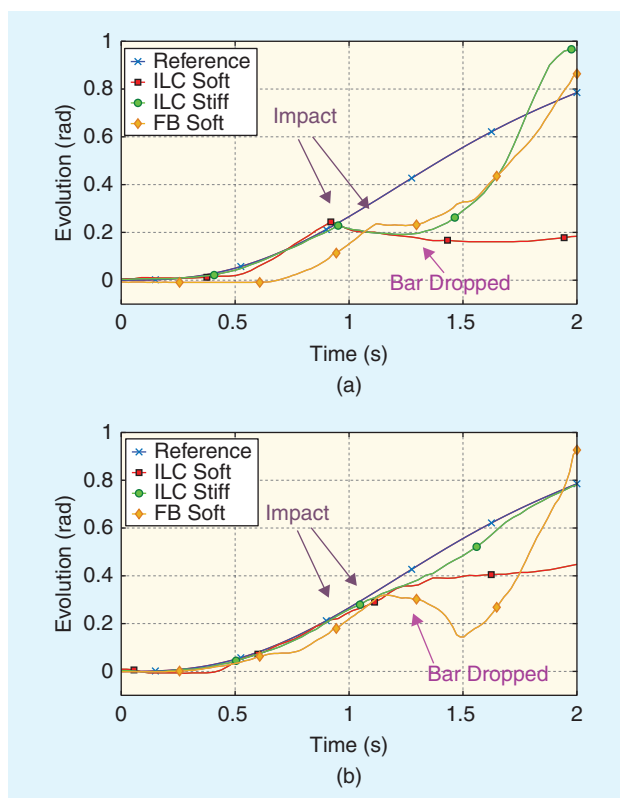


Figure 10. The trajectory followed by a two-DoF horizontal robot in the presence of an obstacle. Panel (a) and panel (b) show, respectively, the trajectories followed by the first and the second joint of the robot. The impact occurs at 0.94 s for the ILC case and at 1.12 s for the high-gain feedback case. For the high-stiffness configuration with the ILC algorithm (ILC Stiff in the legend), the robot drops the bar at 1.3 s and continues to follow the desired trajectory. For the low-stiffness configuration with high-gain feedback action (FB Soft in the legend), the feedback alters the mechanical stiffness, and the robot acts again in a stiff way, dropping the bar. For the low-stiffness configuration with the ILC algorithm (ILC Soft in the legend), the robot maintains its mechanical behavior and adapts to the external environment.

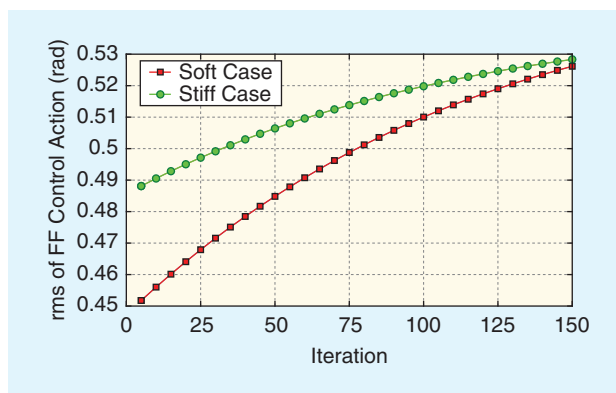


Figure 11. A 2-norm of the feedforward (FF) actions exerted by the proposed controller at each iteration, normalized by the terminal time for low and high stiffness. rms: root-mean-square.

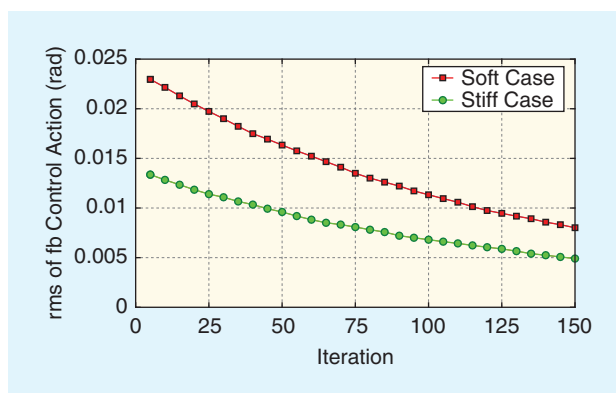


Figure 12. A 2-norm of the feedback actions exerted by the proposed controller at each iteration, normalized by the terminal time for low and high stiffness.

derived conditions to maintain such stiffness alteration under a given threshold. Then we discussed possible approaches to face the introduced problem. Leveraging the human example, we proposed using a suitable combination of low-gain feedback and feedforward, focusing on ILC. Finally, we discussed experiments to prove both the negative effects of high-gain feedback control and the effectiveness of ILC. Interestingly, a gradual shift of control authority from the feedback to the feedforward component was observed.

Acknowledgments

This work is supported by European Commission grant H2020-ICT-645599 (“SOMA”: Soft Manipulation) and European Research Council Advanced grant 291166 (“SoftHands”).

References

[1] D. J. Braun, F. Petit, F. Huber, S. Haddadin, P. Van Der Smagt, A. Albu-Schaffer, and S. Vijayakumar, “Optimal torque and stiffness control in compliantly actuated robots,” in *Proc. IEEE/RSJ Int. Conf. Intelligent Robots and Systems (IROS)*, 2012, pp. 2801–2808.

- [2] D. A. Bristow, M. Tharayil, and A. G. Alleyne, "A survey of iterative learning control," *IEEE Control Syst. Mag.*, vol. 26, no. 3, pp. 96–114, 2006.
- [3] R. W. Brockett, "Minimum attention control," in *Proc. 36th IEEE Conf. Decision and Control*, vol. 3, 1997, pp. 2628–2632.
- [4] R. W. Brockett, "Minimizing attention in a motion control context," in *Proc. 42nd IEEE Conf. Decision and Control*, vol. 4, 2003, pp. 3349–3352.
- [5] M. G. Catalano, G. Grioli, M. Garabini, F. Bonomo, M. Mancini, N. G. Tsagarakis, and A. Bicchi, "VSA-CubeBot: A modular variable stiffness platform for multi degrees of freedom systems," in *Proc. 2011 IEEE Int. Conf. Robotics Automation*, Shanghai, China, May 2011, pp. 5090–5095.
- [6] G. M. Clayton, S. Tien, K. K. Leang, Q. Zou, and S. Devasia, "A review of feedforward control approaches in nanopositioning for high-speed SPM," *J. Dynamic Syst., Measurement, Control*, vol. 131, no. 6, pp. 1–19, 2009.
- [7] S. Devasia, "Should model-based inverse inputs be used as feedforward under plant uncertainty?" *IEEE Trans. Autom. Control*, vol. 47, no. 11, pp. 1865–1871, 2002.
- [8] J. L. Emken, R. Benitez, A. Sideris, J. E. Bobrow, and D. J. Reinkensmeyer, "Motor adaptation as a greedy optimization of error and effort," *J. Neurophysiology*, vol. 97, no. 6, pp. 3997–4006, 2007.
- [9] S. D. Eppinger and W. P. Seering, "Understanding bandwidth limitations in robot force control," in *Proc. IEEE Int. Conf. Robotics Automation*, vol. 4, 1987, pp. 904–909.
- [10] Q. Fu, W. Zhang, and M. Santello, "Anticipatory planning and control of grasp positions and forces for dexterous two-digit manipulation," *J. Neurosci.*, vol. 30, no. 27, pp. 9117–9126, 2010.
- [11] M. Garabini, A. Passaglia, F. Belo, P. Salaris, and A. Bicchi, "Optimality principles in variable stiffness control: The VSA hammer," in *Proc. IEEE/RSJ Int. Conf. Intelligent Robots and Systems (IROS)*, 2011, pp. 3770–3775.
- [12] L. Greco, A. Chaillet, and A. Bicchi, "Exploiting packet size in uncertain nonlinear networked control systems," *Automatica*, vol. 48, no. 11, pp. 2801–2811, 2012.
- [13] M. M. Haith, C. Hazan, and G. S. Goodman, "Expectation and anticipation of dynamic visual events by 3.5-month-old babies," *Child Development*, pp. 467–479, 1988.
- [14] J. P. Hespanha, P. Naghshtabrizi, and Y. Xu, "A survey of recent results in networked control systems," *Proc. IEEE*, vol. 95, no. 1, pp. 138, 2007.
- [15] N. Hogan, "Impedance control: An approach to manipulation: Part II—Implementation," *J. Dynamic Syst., Measurement, Control*, vol. 107, no. 1, pp. 8–16, 1985.
- [16] S. Howard, M. Zefran, and V. Kumar, "On the 6×6 Cartesian stiffness matrix for three-dimensional motions," *Mechanism Machine Theory*, vol. 33, no. 4, pp. 389–408, 1998.
- [17] C. Jang, J. E. Lee, S. Lee, and F. C. Park, "A minimum attention control law for ball catching," *Bioinspiration & Biomimetics*, vol. 10, no. 5, p. 055008, 2015.
- [18] R. S. Johansson and K. J. Cole, "Sensory-motor coordination during grasping and manipulative actions," *Current Opinion Neurobiol.*, vol. 2, no. 6, pp. 815–823, 1992.
- [19] R. S. Johansson and G. Westling, "Coordinated isometric muscle commands adequately and erroneously programmed for the weight during lifting task with precision grip," *Experimental Brain Res.*, vol. 71, pp. 59–71, 1988.
- [20] M. Kawato, "Learning internal models of the motor apparatus," in *The Acquisition of Motor Behavior in Vertebrates*, J. R. Bloedel, T. J. Ebner, and S. P. Wise, Eds. Cambridge, MA: MIT Press, 1996, p. 409.
- [21] M. Kawato, "Internal models for motor control and trajectory planning," *Current Opinion Neurobiol.*, vol. 9, no. 6, pp. 718–727, 1999.
- [22] S. Kim, C. Laschi, and B. Trimmer, "Soft robotics: A bioinspired evolution in robotics," *Trends Biotechnol.*, vol. 31, no. 5, pp. 287–294, 2013.
- [23] K. P. Kording and D. M. Wolpert, "Bayesian integration in sensorimotor learning," *Nature*, vol. 427, no. 6971, pp. 244–247, 2004.
- [24] J. W. Krakauer and P. Mazzoni, "Human sensorimotor learning: Adaptation, skill, and beyond," *Current Opinion Neurobiol.*, vol. 21, no. 4, pp. 636–644, 2011.
- [25] F. Lacquaniti, F. Licata, and J. F. Soechting, "The mechanical behavior of the human forearm in response to transient perturbations," *Biol. Cybern.*, vol. 44, no. 1, pp. 35–46, 1982.
- [26] F. Lacquaniti and C. Maioli, "The role of preparation in tuning anticipatory and reflex responses during catching," *J. Neurosci.*, vol. 9, no. 1, pp. 134–148, 1989.
- [27] J. H. Lee, "Model predictive control: Review of the three decades of development," *Int. J. Control, Autom. Syst.*, vol. 9, no. 3, pp. 415–424, 2011.
- [28] L. Marconi, L. Praly, and A. Isidori, "Output stabilization via nonlinear Luenberger observers," *SIAM J. Control Optimization*, vol. 45, no. 6, pp. 2277–2298, 2007.
- [29] N. C. Martins and M. Dahleh, "Feedback control in the presence of noisy channels: bode-like fundamental limitations of performance," *IEEE Trans. Autom. Control*, vol. 53, no. 7, pp. 1604–1615, 2008.
- [30] R. Osu, D. W. Franklin, H. Kato, H. Gomi, K. Domen, T. Yoshioka, and M. Kawato, "Short- and long-term changes in joint co-contraction associated with motor learning as revealed from surface EMG," *J. Neurophysiology*, vol. 88, no. 2, pp. 991–1004, 2002.
- [31] P. R. Ouyang, B. A. Petz, and F. F. Xi, "Iterative learning control with switching gain feedback for nonlinear systems," *J. Computational Nonlinear Dynamics*, vol. 6, no. 1, pp. 011020, 2011.
- [32] P. Gianluca, M. Claudio, and D. L. Alessandro, "On the feedback linearization of robots with variable joint stiffness," in *Proc. IEEE Int. Conf. Robotics Automation (ICRA)*, 2008, pp. 1753–1759.
- [33] R. Pfeifer and G. Gómez, "Morphological computation—connecting brain, body, and environment," in *Creating Brain-Like Intelligence*, B. Sendhoff, E. Körner, O. Sporns, H. Ritter, and K. Doya, Eds. Berlin, Germany: Springer-Verlag, 2009, pp. 66–83.
- [34] G. Pratt and M. M. Williamson, "Series elastic actuators," in *Proc. IEEE/RSJ Int. Conf. Intelligent Robots and Systems (Human Robot Interaction and Cooperative Robots)*, vol. 1, 1995, pp. 399–406.
- [35] S. Schaal and C. Atkeson, "Learning control in robotics," *IEEE Robot. Autom. Mag.*, vol. 17, no. 2, pp. 20–29, 2010.
- [36] L. Sciacivico and B. Siciliano, *Modelling and Control of Robot Manipulators*. London, U.K.: Springer-Verlag, 2000.
- [37] R. Shadmehr and F. A. Mussa-Ivaldi, "Adaptive representation of dynamics during learning of a motor task," *J. Neurosci.*, vol. 14, no. 5, pp. 3208–3224, 1994.
- [38] G. Tonietti and A. Bicchi, "Adaptive simultaneous position and stiffness control for a soft robot arm," in *Proc. IEEE/RSJ Int. Conf. Intelligent Robots and Systems*, vol. 2, 2002, pp. 1992–1997.
- [39] M. H. van der Linden, D. S. Marigold, F. J. M. Gabreëls, and J. Duyens, "Muscle reflexes and synergies triggered by an unexpected support surface height during walking," *J. Neurophysiology*, vol. 97, no. 5, pp. 3639–3650, 2007.

[40] B. Vanderborght, A. Albu-Schäffer, A. Bicchi, E. Burdet, D. G. Caldwell, R. Carloni, M. Catalano, O. Eiberger, W. Friedl, G. Ganesh, and M. Garabini, "Variable impedance actuators: A review," *Robot. and Auton. Syst.*, vol. 61, no. 12, pp. 1601–1614, 2013.

[41] D. M. Wolpert, J. Diedrichsen, and J. Randall Flanagan, "Principles of sensorimotor learning," *Nature Rev. Neurosci.*, vol. 12, no. 12, pp. 739–751, 2011.

Cosimo Della Santina Enrico Piaggio Research Center, University of Pisa, Italy. E-mail: cosimodellasantina@gmail.com.

Matteo Bianchi, Enrico Piaggio Research Center, University of Pisa, Italy. E-mail: matteobianchi23@gmail.com.

Giorgio Grioli, Department of Advanced Robotics, Istituto Italiano di Tecnologia, Genoa, Italy. E-mail: giorgio.grioli@gmail.com.

Franco Angelini, Enrico Piaggio Research Center, University of Pisa, Italy and Department of Advanced Robotics, Istituto Italiano di Tecnologia, Genoa, Italy. E-mail: frncangelini@gmail.com.

Manuel Catalano, Department of Advanced Robotics, Istituto Italiano di Tecnologia, Genoa, Italy. E-mail: manuel.catalano@iit.it.

Manolo Garabini, Enrico Piaggio Research Center, University of Pisa, Italy. E-mail: manolo.garabini@gmail.com.

Antonio Bicchi, Enrico Piaggio Research Center, University of Pisa, Italy, and Department of Advanced Robotics, Istituto Italiano di Tecnologia, Genoa, Italy. E-mail: antonio.bicchi@unipi.it.

